S1. Elemental analysis of powder samples

Elemental analysis (O, C, H, N, S) was performed in a Thermo Flash 1112 analyzer. Determination of metals (Al, Co, Mo, Ni, Y) was performed by Induction Coupled Plasma (ICP) spectroscopy. Samples were processed with sodium peroxide and analyzed in a Spectroblue spectrometer by Ametek.

Table S1. Elemental analysis: all the data are provided in wt.%.

Material	O	C	H	N	S	Metals	Rest
MWCNT	0.9	89.9	0.3	0.1	0.0	4.9[a]	3.9
CVD-SWCNT	5.7	86.2	0.5	0.5	0.0	0.1 + 0.6 + 4.0[b]	2.5
AD-SWCNT	2.5	69.5	0.3	0.4	1.6	17.3 + 5.18[c]	3.2
c-HNO_3-MWCNT	8.6	90.1	0.4	0.3	0.0	0.0[a]	0.6
d-HNO_3-MWCNT	3.7	90.5	0.7	1.0	0.0	2.0[a]	2.1
F-MWCNT	8.1	83.2	0.5	0.5	0.0	4.3[a]	3.5
HSO_3-MWCNT	6.5	80.4	1.0	1.7	1.1	3.8[a]	5.5
GO-2	38.8	47.2	2.8	0.1	1.1	-	9.9
GO-4	42.6	41.5	3.3	0.0	1.0	-	11.6
GO-16	46.0	40.8	3.1	0.0	1.4	-	8.8
GO-G[a]	42.0	46.7	2.7	2.4	2.3	-	3.9

[a] Aluminum

[b] Aluminum, cobalt, and molybdenum

[c] Nickel and Yttrium

S2. Analysis of dispersion quality

Stability parameters of CNT and GO dispersions are included in Table S2. The centrifugation yield (Y_{cf}) was calculated from optical absorbance measurements (Figure S1). Zeta potential (ζ) and zeta-size measurements were performed in a Z-Sizer Nano by Malvern. The ζ values are calculated from determinations of the electrophoretic mobility in U-shaped polymeric cells by Malvern. The zeta-size was determined in polymeric cuvettes from Malvern.

Optical absorption spectroscopy was performed in Shimadzu UV-2401 PC and FTIR Vertex 70 Bruker spectrometers. Liquid dispersions were measured in quartz cuvettes of 1 cm optical path. The instrument baseline was carefully checked before each experimental session, so that changes in the absorbance can be quantitatively associated to changes in concentration. Spectrum profiles of CNT and GO dispersions are shown in Figure S1. The change in concentration was calculated as the absorbance ratio, before

and after the centrifugation process, at a wavelength of 850 nm and 550 nm respectively for CNT and GO dispersions.

Table S2. Stability parameters of CNT and GO suspensions: starting concentration (C_0), yield of centrifugation (Y_{cf}), zeta potential (ζ), pH, and zeta-size in radius (r_z).

Dispersion	C_0 **[mg·mL^{-1}]**	Y_{cf} **[%]**	ζ **[mV]**	**pH**	r_z **[nm]**
Water					
GO-2	2	25	-44.0	2.6	231
GO-4	2	52	-42.2	2.5	188
GO-16	2	100	-42.0	2.5	632
GO-G[a]	4	100	-42.1	1.8	604
HSO_3-MWCNT	2	46	-31.9	7.2	-
0.5% SDBS					
MWCNT	0.4	57	-43.7	7.8	-
MWCNT	1	67	-42.5	8.2	-
MWCNT	2	75	-45.8	7.8	118
MWCNT	4	84	-44.5	7.9	-
c-HNO_3-MWCNT	2	93	-48.6	7.0	98
d-HNO3-MWCNT	2	79	-46.2	7.3	101
F-MWCNT	2	91	-47.8	7.4	59
HSO_3-MWCNT	2	82	-49.3	7.5	105
CVD-SWCNT	2	82	-58.6	6.8	147
AD-SWCNT	2	90	-58.7	9.0	70
20% Solsperse					
MWCNT	0.4	77	-4.1	7.0	-
MWCNT	1	67	-4.4	6.9	-
MWCNT	2	58	-4.2	7.0	-
MWCNT	4	59	-4.0	7.0	-

[a]The provider does not specify the presence of additives for improving GO stability in water.

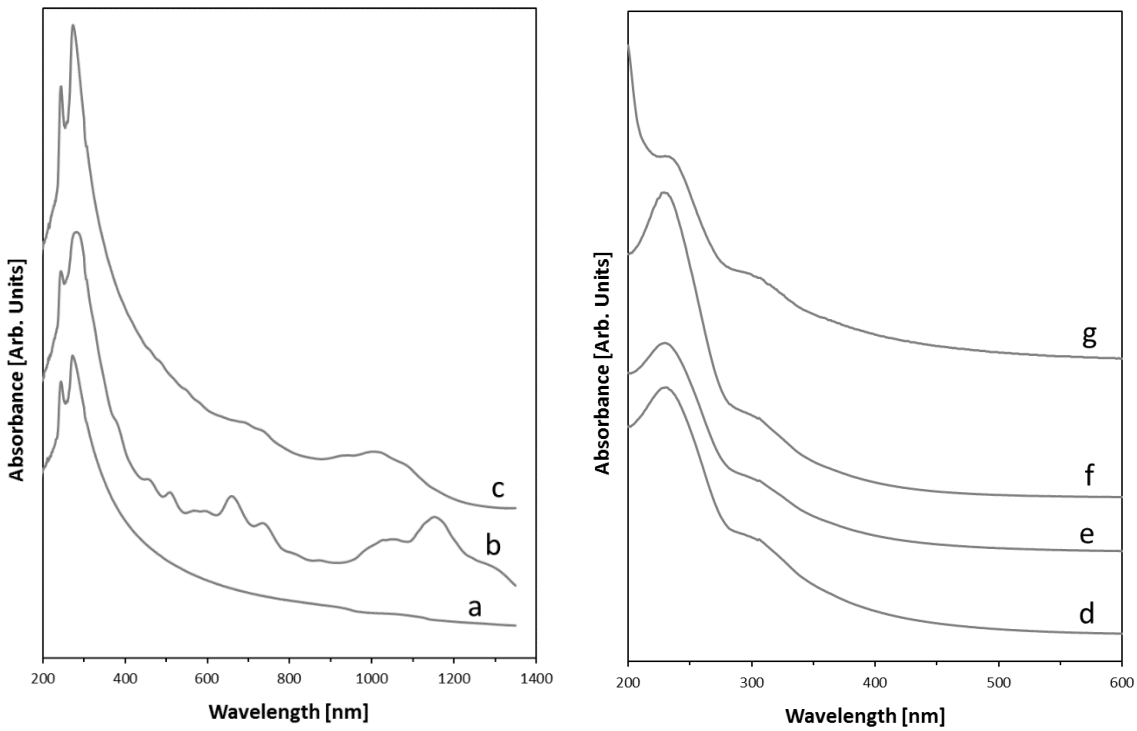

Figure S1. Absorption spectra of CNT dispersions in 0.5% SDBS and GO dispersions in water: a) MWCNT, b) CVD-SWCNT, c), AD-SWCNT, d) GO-2, e) GO-4, f) GO-16, and g) GO-G.

The centrifugation yield (Y_{cf}) is a typical parameter for the assessment of stability in colloids. The SWCNT dispersions in SDBS gave very high Y_{cf}, in the range of 80-90%. Comparatively, the MWCNT dispersion in SDBS led to a lower average Y_{cf} of 71%, which still indicates a quite high stability. In the other surfactant (Solsperse), the stability of MWCNTs was relatively high too, with an average Y_{cf} of 65%, approaching values of the SDBS surfactant. The Y_{cf} of the f-CNT suspensions in SDBS was in the range of 82-93%, being higher than that for pristine MWCNTs. The Y_{cf} value for the HSO_3-MWCNT material in water was also relatively high (46%). Among the GO samples, the Y_{cf} for GO-2 is only 25%, indicating that most of the powder sample was not oxidized enough to be stable in water. The effect of oxidation is evidenced by the increase to 52% in Y_{cf} for GO-4. Centrifugation of GO-16 and GO-G did not show any apparent sedimentation; therefore they were not centrifuged for the present work (Y_{cf} = 100%).

Stability in colloids is associated to two main causes: steric factors (also called entropic or excluded volume factors) and electrostatic stabilization. The electrostatic component can be approximated in a semi-quantitative way by measuring the zeta potential (ζ). The ζ values of GO and CNT dispersions after centrifugation are presented in Figure S2. For

GO dispersions in water, ζ values are in the range of -42 to -44 mV, which corresponds to a quite high level of electrostatic stability. The negative sign of ζ is associated to negative charges on the abundant oxygen chemical groups of GO. Despite the low Y_{cf} that was observed after centrifugation of the GO-2 dispersion, the electrostatic stability of the remaining supernatant is like that of the other GO dispersions.

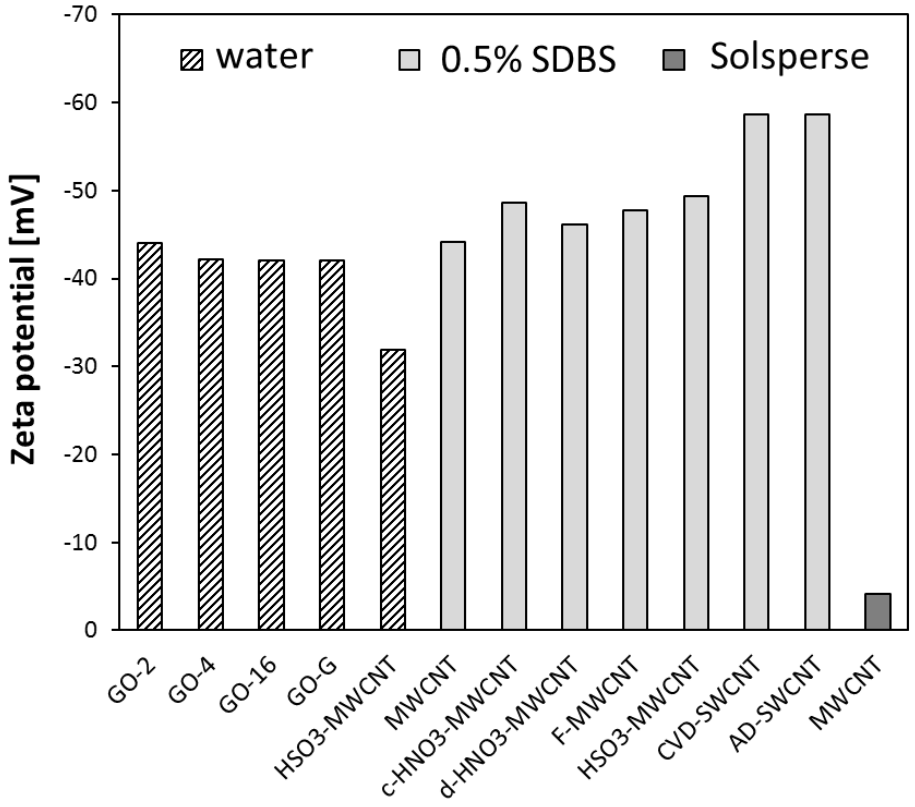

Figure S2. Zeta potential of GO and CNT dispersions in water, 0.5% SDBS and 20% Solsperse.

The ζ values of both CVD- and AD-SWCNT dispersions in SDBS are very high, reaching -59 mV, while the average ζ of pristine MWCNT dispersions is around -49 mV. The negative sign of ζ in CNT dispersions derive from the surfactant anions that are adsorbed on CNTs. The high ζ values in SWCNTs might be due to their high aspect ratio and thus high specific surface area for surfactant adsorption. Opposite to the SDBS medium, MWCNT dispersions in Solsperse show very low ζ values around -4.2 mV. Although sedimentation experiments proved that Y_{cf} in SDBS and Solsperse are similar, the electrostatic contribution of Solsperse to stability is very low, suggesting that CNT dispersions in Solsperse are mainly stabilized by steric interactions.

The ζ values for f-MWCNT dispersions in SDBS are in the range of -46 to -50 mV, being somewhat higher than for pristine MWCNTs. Therefore, chemical functionalization increases the electrostatic stability of the colloid, in agreement with the above observed increase in the Y_{cf}. The ζ value depends on the functionalization strategy: HSO_3-MWCNT > c-HNO_3-MWCNT > F-MWCNT > d-HNO_3-MWCNT > MWCNT. Also, the HSO_3-MWCNT sample can be directly dispersed in water with a quite high ζ value of -32 mV.

Another parameter that can be related to the dispersion quality is the effective hydrodynamic size (zeta-average size). The zeta-size for GO and CNT dispersions was measured by dynamic light scattering (DLS). The most common DLS technique is strictly valid only for spherical particles; with high aspect ratio nanoparticles, it can be used in a semi-quantitative way for the calculation of an equivalent hydrodynamic size. The zeta-size is mainly associated with two characteristics of colloids: the particle size, and the degree of aggregation, which tends to a minimum in high quality dispersions. The zeta-size of GO dispersions is high because GO flakes are quite large, as it will be discussed later in this work.

The zeta-size of GO-16 and GO-G (632 and 604 nm in radius respectively) is substantially higher than in GO-2 and GO-4 dispersions (231 and 188 nm). However, it has to be reminded that only the last two were processed by centrifugation. The zeta-size of pristine CNT dispersions, in the range of 70-118 nm, is smaller than in GO. For f-CNTs, the zeta-size decreases from 118 to 59-105 nm. The decrease can be associated both to a decrease in CNT length by breakage and to a decrease in the aggregation level by the improvement in the electrostatic stability.

In summary, all the studied GO and CNT dispersions show a good colloidal stability for viscosity measurements, but with some differences in ζ values and zeta-size. The ζ value depends on the CNT type and functionalization, and drastically decreases in the Solsperse surfactant. The zeta-size for GO samples is much higher than for CNT samples.

S3. Kinematic viscosity of CNT and GO dispersions

Table S3. Kinematic viscosity (ν) of CNT and GO dispersions at various concentrations (C) and 5 temperatures in 3 liquid media: water, 0.5% SDBS and 20% Solsperse.

Dispersion	C **[mg·mL^{-1}]**	ν **[mm^2·s^{-1}]**				
		298.15 K	303.15 K	308.15 K	313.15 K	318.15 K
Water						
---	---	0.893	0.801	0.724	0.658	0.604
GO-2	0.50	1.043	0.940	0.848	0.770	0.702
GO-4	1.04	1.564	1.415	1.275	1.157	1.053
GO-16	2.00	1.720	1.555	1.321	1.264	1.152
GO-16	4.00	4.002	3.593	3.201	2.988	2.730
GO-G	2.00	1.788	1.613	1.469	1.301	1.190
GO-G	4.00	3.335	2.994	2.678	2.421	2.194
HSO_3-MWCNT	0.91	0.987	0.928	0.856	0.799	0.757
0.5% SDBS						
---	---	0.912	0.825	0.746	0.674	0.617
MWCNT	0.23	0.938	0.853	0.766	0.695	0.639
MWCNT	0.67	0.980	0.887	0.798	0.727	0.667
MWCNT	1.51	1.060	0.951	0.861	0.786	0.716
MWCNT	3.35	1.217	1.084	0.966	0.889	0.815
c-HNO_3-MWCNT	1.86	1.034	0.948	0.848	0.769	0.704
d-HNO3-MWCNT	1.57	1.053	0.960	0.862	0.785	0.724
F-MWCNT	1.81	1.043	0.949	0.851	0.771	0.704
HSO_3-MWCNT	1.64	1.023	0.934	0.836	0.765	0.700
CVD-SWCNT	1.64	2.808	2.567	2.321	2.115	1.951
AD-SWCNT	1.80	1.077	0.975	0.878	0.800	0.729
20% Solsperse						
---	---	4.127	3.564	3.067	2.675	2.333
MWCNT	0.31	4.557	3.934	3.397	2.986	2.612
MWCNT	0.67	5.210	4.576	3.908	3.692	3.192
MWCNT	1.16	6.145	5.310	4.855	4.524	3.885

S4. Density of CNT and GO dispersions

Density (ρ) measurements were performed in a 5 mL pycnometer (Blaubrand). The determined ρ values are listed in Table S4, being approximately constant with the addition of nanoparticles. The absolute viscosity (η) can be calculated as $\eta = \nu \cdot \rho$.

Table S4. Density (ρ) of CNT and GO dispersions at ambient temperature (T_a) and pressure.

Sample	C [mg·mL^{-1}]	T_a [K]	ρ [g·cm^{-3}]
Water			
---	---	296.75	0.9967
GO-2	1.04	299.25	0.9961
GO-4	0.44	299.25	0.9962
GO-16	2.00	299.25	0.9961
GO-G	4.00	289.25	0.9984
HSO_3-MWCNT	0.91	296.75	0.9959
0.5% SDBS			
---	---	296.75	0.9967
MWCNT	0.23	296.75	0.9969
MWCNT	0.67	296.75	0.9979
MWCNT	1.51	296.75	0.9987
MWCNT	3.35	296.75	0.9995
c-HNO_3-MWCNT	1.86	296.75	0.9979
d-HNO3-MWCNT	1.57	289.75	0.9991
F-MWCNT	1.81	289.85	0.9987
HSO_3-MWCNT	1.64	296.75	0.9979
CVD-SWCNT	1.64	289.85	0.9976
AD-SWCNT	1.80	289.85	0.9986
20% Solsperse			
---	---	296.75	1.0305
MWCNT	0.31	296.75	1.0332
MWCNT	0.67	296.75	1.0336
MWCNT	1.16	296.75	1.0337
MWCNT	2.35	296.75	1.0339

S5. Dependence of relative viscosity with temperature

In Figures S3-S5, the relative viscosity (v_r) is calculated as the ratio between experimental measurements for nanoparticle dispersions and the respective aqueous media. The v_r values are approximately constant in the measured temperature range. Certain deviations are only observed for MWCNT dispersions in Solsperse (Figure S5).

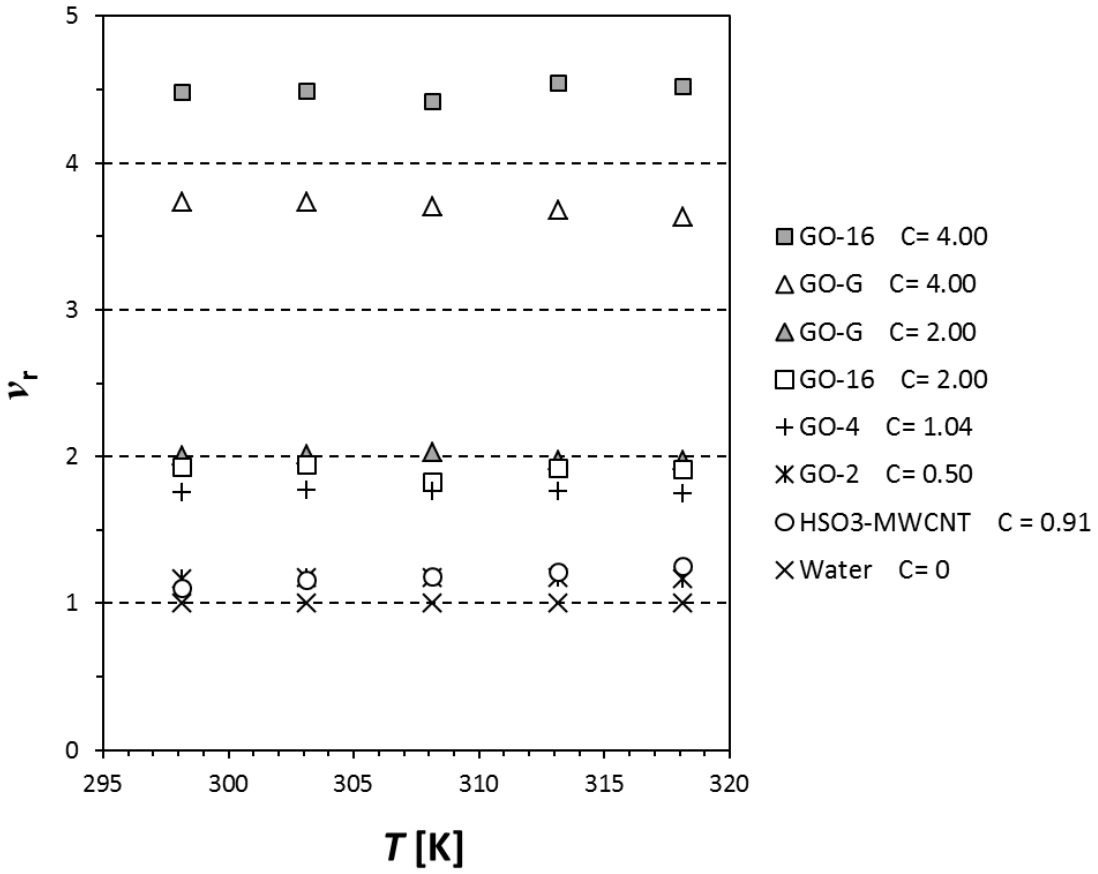

Figure S3. Relative viscosity (v_r) at 5 temperatures for various dispersions of GO and HSO_3-MWCNT materials in water.

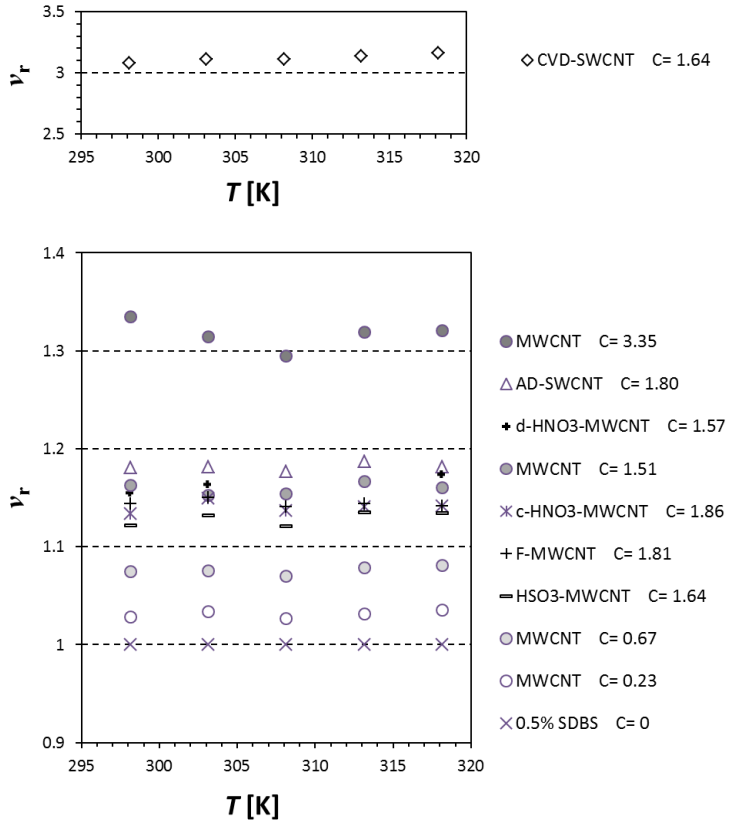

Figure S4. Relative viscosity (v_r) at 5 temperatures for various dispersions of CNT and functionalized CNT materials in 0.5% SDBS.

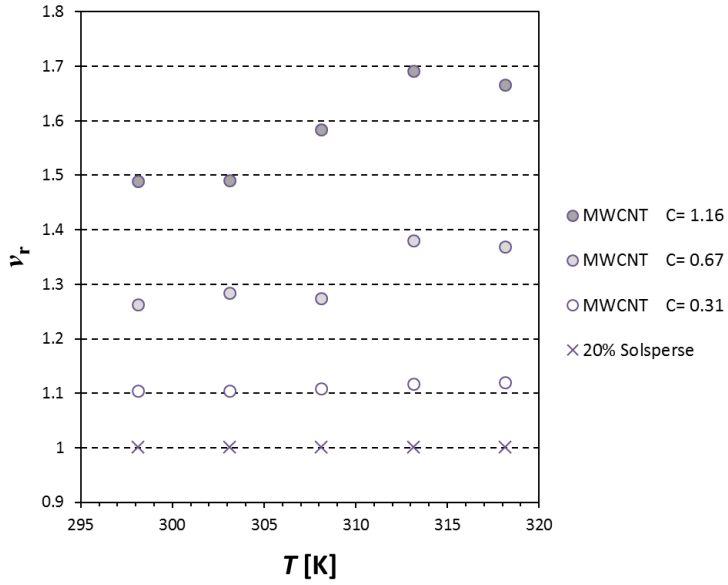

Figure S5. Relative viscosity (v_r) at 5 temperatures for various dispersions of MWCNTs in 20% Solsperse.

S6. The Maron and Pierce equation for non-Newtonian suspensions

According to the generalized model of Maron and Pierce, the viscosity of a suspension of solid spherical particles in a fluid is given by a two-term equation:

$$\eta = \frac{K_a^0}{(1-\epsilon_a\phi)^2} e^{\Delta H_1^*/RT} + \frac{K_b^0(\epsilon_b\phi)^2}{(1-\epsilon_b\phi)^3} e^{\Delta H_b^*/RT} \frac{senh^{-1}\beta(\phi,T)G}{\beta(\phi,T)G} \qquad \text{(Eq. S1)}$$

where T is the temperature, ϕ is the volume fraction of nanoparticles, $\beta(\phi,T)$ is a function of both variables, G is the rate of shear, and the other coefficients are constants. The factor [senh^{-1} $\beta(\phi,T)G/\ \beta(\phi,T)G$] accounts for the non-Newtonian behavior. In a Newtonian fluid, the factor is constant an equals 1.

The relative viscosity is:

$$\eta_r = \frac{1}{(1-\epsilon_a\phi)^2} + \frac{A(\epsilon_b\phi)^2}{(1-\epsilon_b\phi)^3} e^{\Delta H^*/RT} \frac{senh^{-1}\beta(\phi,T)G}{\beta(\phi,T)G} \qquad \text{(Eq. S2)}$$

with $A = K_b^0/K_a^0$ and $\Delta H^* = \Delta H_b^* - \Delta H_1^*$.

In order to evaluate the relevance of the second term in Equation S2, experimental η_r data were analyzed. More specifically, the second term accounts for the dependence on temperature and corrects the contribution of the concentration. Figures S3-S5 show that the η_r does not substantially change with temperature in the considered measurement range. Besides, by considering the second term in Equation S2, two extra parameters (A and ϵ_b) take part in the mathematical fitting; however, the fitting of our experimental data to the model does not improve significantly.

S7. Fitting parameters of Equation 1

Table S5. Fitting parameters of the Maron-Pierce model (Equation 1).

Dispersion	K_a^0 [mm^2·s^{-1}]	ϵ [mL·mg^{-1}]	$\Delta H_1^*/R$ [K]
Water			
GO-2	0.00164	0.1500	1877
GO-4	0.00164	0.2359	1878
GO-16	0.00184	0.1321	1844
GO-G	0.00121	0.1207	1977
HSO_3-MWCNT	0.00499	0.0884	1535
0.5% SDBS			
MWCNT	0.00172	0.0396	1873
c-HNO_3-MWCNT	0.00180	0.0341	1857
d-HNO3-MWCNT	0.00195	0.0461	1832
F-MWCNT	0.00170	0.0359	1875
HSO_3-MWCNT	0.00190	0.0358	1839
CVD-SWCNT	0.00246	0.2645	1761
AD-SWCNT	0.00178	0.0444	1860
20% Solsperse			
MWCNT	0.00161	0.1788	2328

S8. Accuracy of viscosity measurements in MWCNT/SDBS and MWCNT/ Solsperse systems

In the main text of the article, it is stated that ΔH_1^* is only dependent on the liquid medium, but not on the type and concentration of the nanoparticles in suspension. Therefore, according to the model of Maron and Pierce, ΔH_1^* values are expected to be identical for all the nanoparticle concentrations, including the pure liquid medium (C = 0 mg·mL^{-1}). Indeed, Figure S6.a shows that ΔH_1^* for different concentrations of MWCNTs in 0.5% SDBS is constant with an accuracy of 3%.

However, the plot of ln (v) vs. 1/T for MWCNTs in 20% Solsperse (Figure S6.b) indicates different ΔH_1^* values, decreasing with the MWCNT concentration. In the following, we analyze possible reasons for the trend in ΔH_1^* values:

a) First, the validity of the simplified Maron-Pierce equation for the MWCNT/Solsperse system was reconsidered. To check possible effects of non-Newtonian behavior, equation S1 was tried for data fitting instead of the simplified Equation 1. It was confirmed that the fitting does not improve substantially.

b) As it is commented in the main text, the zeta-potential in MWCNT/Solsperse dispersions is very low, and the stability is likey related to steric factors. Therefore, an influence of entropy might be considered. The variations of enthalpy and entropy are related by the formulae $\Delta H = T\Delta S$. Thus, a change in ΔS due to steric factors would result in a mere multiplicative constant factor in η. It would bring about a vertical shift in the ln (η) vs. 1/T plot, but it would not influence its slope. Consequently, such a change is ruled out as an explanation for the observed behavior of ΔH_1^* in the considered sample.

c) Next, we consider the accuracy of viscosity measurements. Figure S7 shows the plot of ln (η) vs. 1/T with a linear trend that was calculated using the Maron-Pierce parameters K_a^*, ϵ and ΔH_1^* from Table S5. Now the parameters are common for all the measured concentrations in 2% Solsperse. The model agrees quite well with experimental data, considering an accuracy of 5% in the measurements.

d) Finally, it is possible that ΔH_1^* really changes with MWCNT concentration. According to the Maron-Pierce model, the change would indicate an indirect effect on the molecular interactions in the liquid medium. However, a complete discussion at the molecular level is out of the scope of this work.

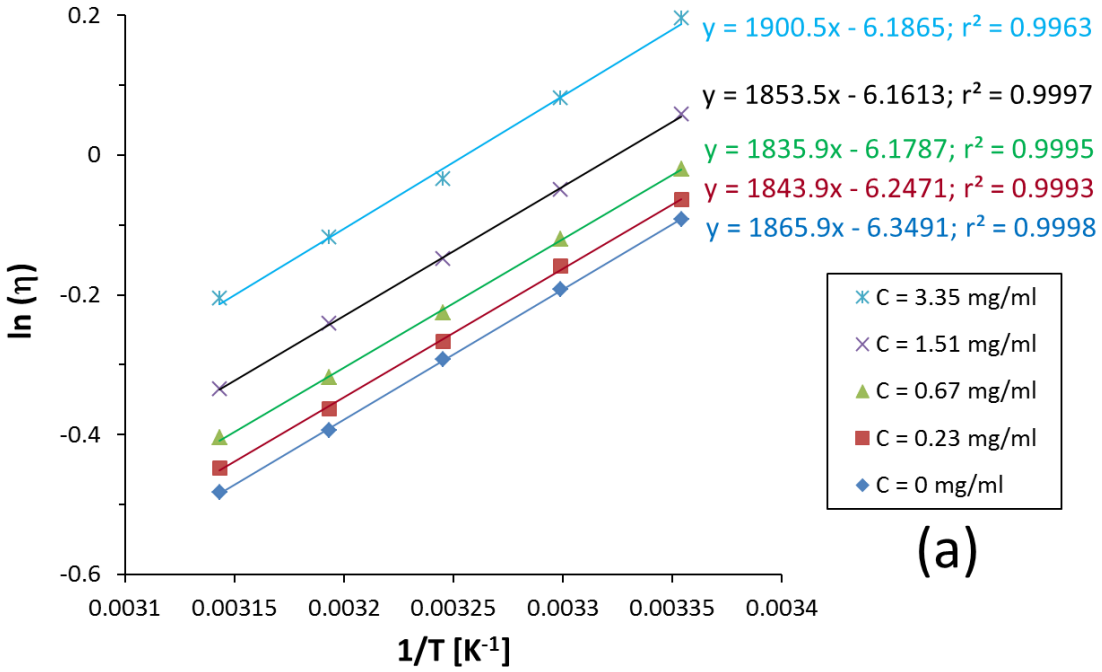

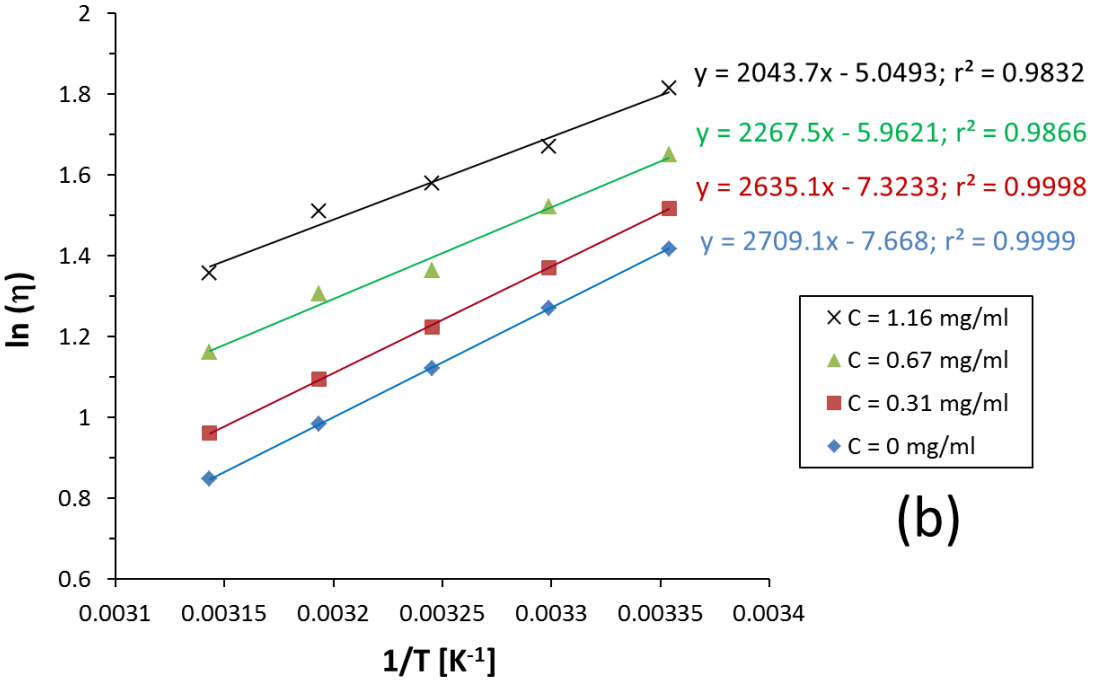

Figure S6. Calculation of $\Delta H_1^*/R$ at different MWCNT concentrations in: a) 0.5% SDBS and b) 20% Solsperse.

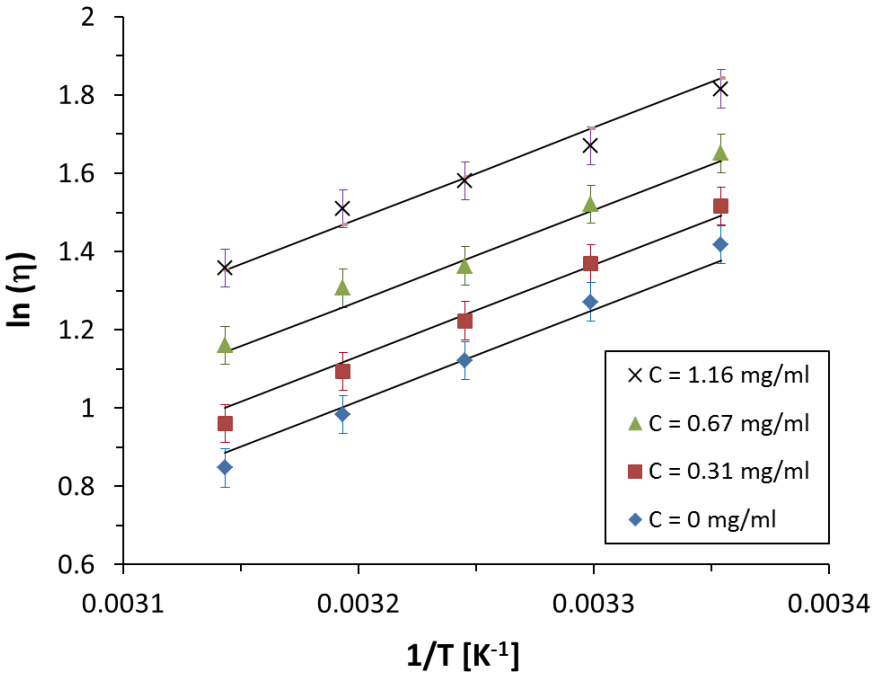

Figure S7. Plot of ln (η) vs. 1/T for MWCNT dispersions in 20% Solsperse. The fitting lines were calculated applying the Maron-Pierce equation with K_a^0, ϵ and ΔH_1^* parameters from Table S5. The error bars represent an accuracy of 5% in viscosity measurements.

S9. Calculation of the particle density (ρ_p) of CNTs and GO

The specific surface area (*SSA*) of graphene sheets and CNTs can be calculated only from structural and geometric parameters (Table S6, Ref. 46). For simplicity, oxygen chemical groups on both CNTs and GO are neglected in the geometry discussion. The quantity of oxygen, other heteroatoms and impurities will be taken into account later in the calculation of ϕ_m and the intrinsic viscosity. Similarly to *SSA*, the volumetric density of the nanoparticle (ρ_p) can be calculated from geometric parameters (Table S7).

Table S6. Structural and geometric parameters of graphene and CNTs.

Parameter	Description	Value
m_C	Mass of a carbon atom	$1.99447 \cdot 10^{-23}$ g
D_C	Diameter of a carbon atom	---
d_{CC}	Distance between carbon atoms	0.1421 nm
n_L	Number of layers	7 (MWCNTs) Table 5 (GOs)
d_{LL}	Distance between layers	0.34 nm (MWCNTs) Table 5 (GOs)
D	External diameter of a CNT	Table 2

Table S7. Formulae for the calculation of *SSA* and ρ_p.

Nanoparticle	*SSA*	ρ_p
Graphene	$SSA_G = \frac{3\sqrt{3}}{4}\frac{d_{CC}^2}{m_C}$	$\frac{1}{D_C \cdot SSA_G}$
SWCNT	$SSA_{SWCNT} = SSA_G$	$\frac{4}{D \cdot SSA_G}$
MWCNT	$SSA_{MWCNT} = \frac{D \cdot SSA_G}{Dn_L - n_L(n_L - 1)d_{LL}}$	$\frac{4}{D \cdot SSA_{MWCNT}}$
GO	$SSA_{GO} = \frac{SSA_G}{n_L}$	$\frac{n}{(n-1) \cdot d_{LL} \cdot SSA_G}$

S10. Scanning electron microscopy: distribution of CNT lengths and GO surface areas

Scanning electron microscopy (SEM) images were performed in either a field emission SEM model MERLIN (Carl Zeiss, Switzerland) or a SEM EDX Hitachi S-3400N equipment. Stainless-steel sample holders were polished and used as the supports. The CNT and GO dispersions were diluted and drop-casted on the sample holders at approximately 80ºC. The samples were washed by immersion of the sample holders in deionized water to remove, as far as possible, the SDBS surfactant and other impurities from GO synthesis. Representative SEM images of all the samples are shown in Figures S8-S10. Various SEM images of each sample were enlarged and the nanoparticles were individually measured. The resulting distributions are presented in Figures S11-13.

The length of individual CNTs and the surface area of GO flakes vary in a rather wide range. In this work, both variables are assumed to follow a log-normal distribution. When a series of values {x} follows a log-normal distribution, the series {y = ln (x)} follows a normal (Gaussian) distribution, whose average and standard deviation are respectively μ and σ. The density of probability P(x) is given by:

$$P(x) = \frac{1}{\sqrt{2\pi}\sigma x} \exp\left(-\frac{(\ln(x) - \mu)^2}{2\sigma^2} \right) \quad \text{(Eq. S3)}$$

According to the theory of probability distributions, the μ and σ parameters can be calculated by fitting the experimental distribution of CNT lengths and GO areas to the log-normal distribution. After that, average (x_a) and median (x_m) values can be calculated as:

$$x_a = exp\left(\frac{\sigma^2}{2} + \mu\right) \quad \text{(Eq. S4)}$$

$$x_m = e^{\mu} \quad \text{(Eq. S5)}$$

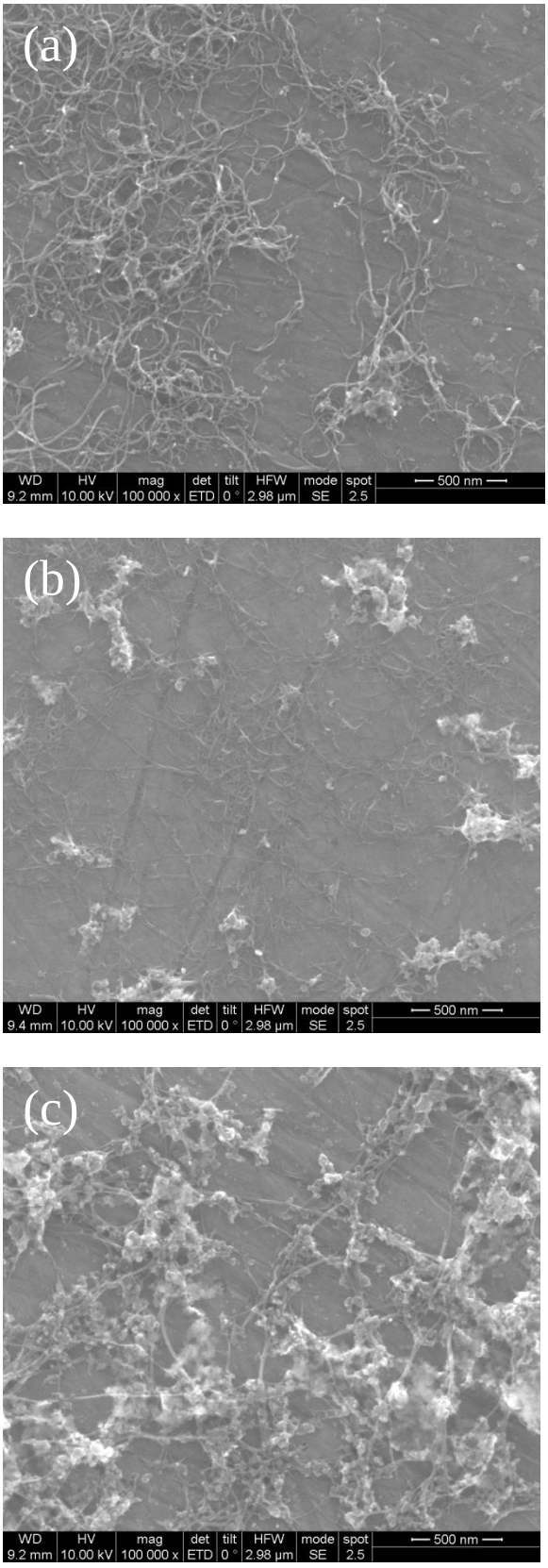

Figure S8. SEM images of the CNT samples: a) MWCNT, b) CVD-SWCNT, and c) AD-SWCNT.

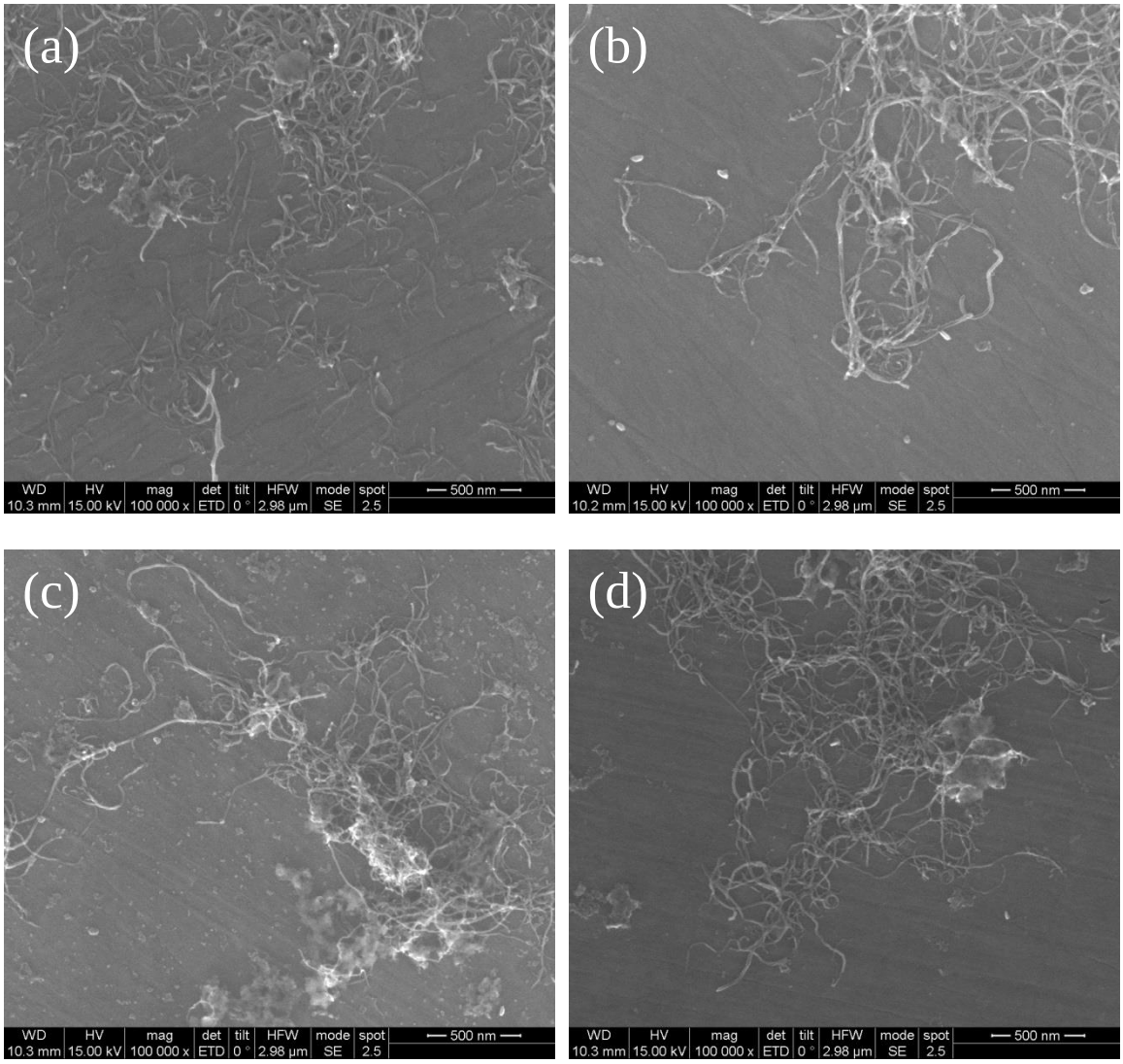

Figure S9. SEM images of the functionalized MWCNT samples: a) c-HNO_3-MWCNT, b) d-HNO_3-MWCNT, c) F-MWCNT, and d) HSO_3-MWCNT.

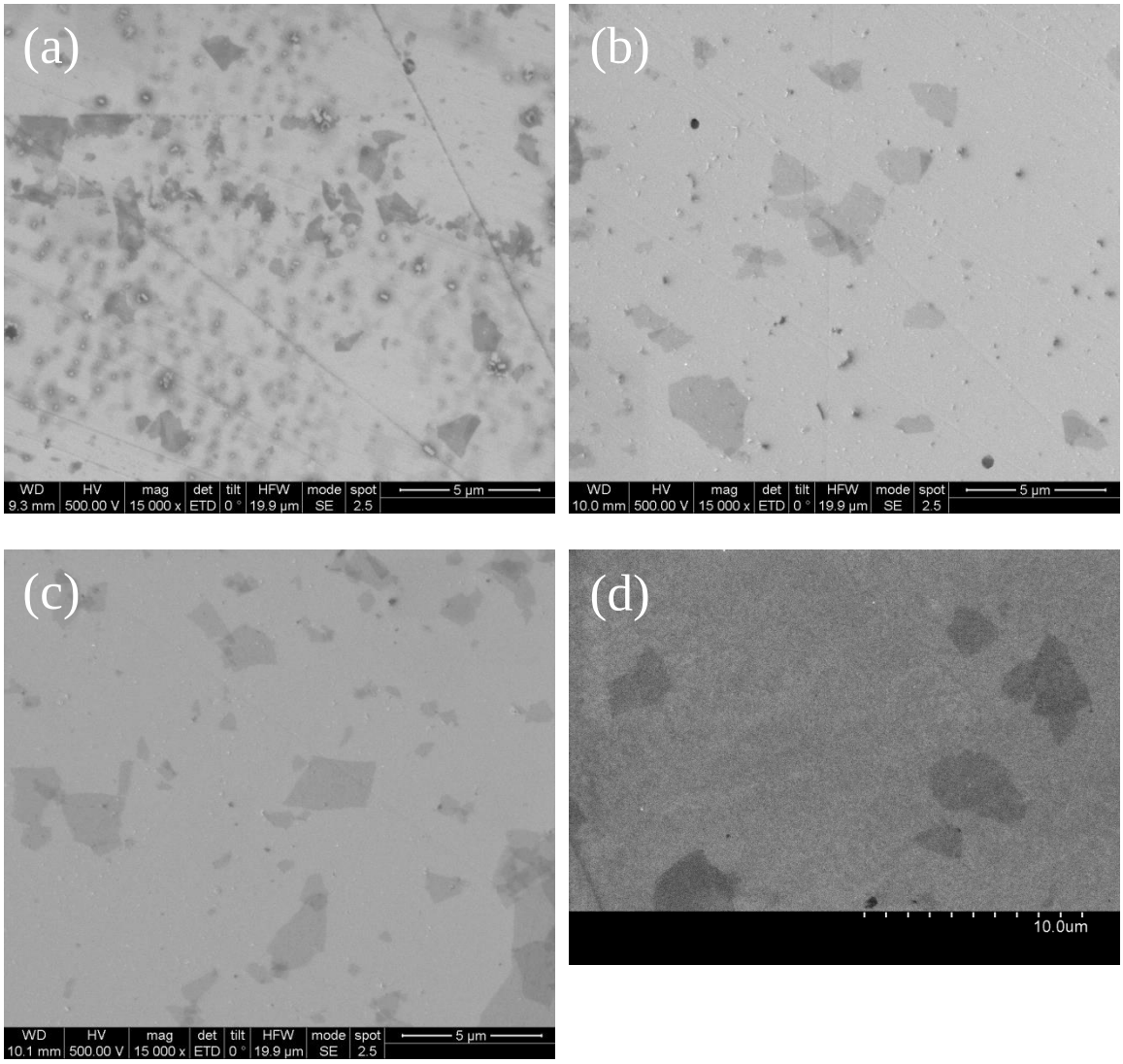

Figure S10. SEM images of the GO samples: a) GO-2, b) GO-4, c) GO-16 and d) GO-G.

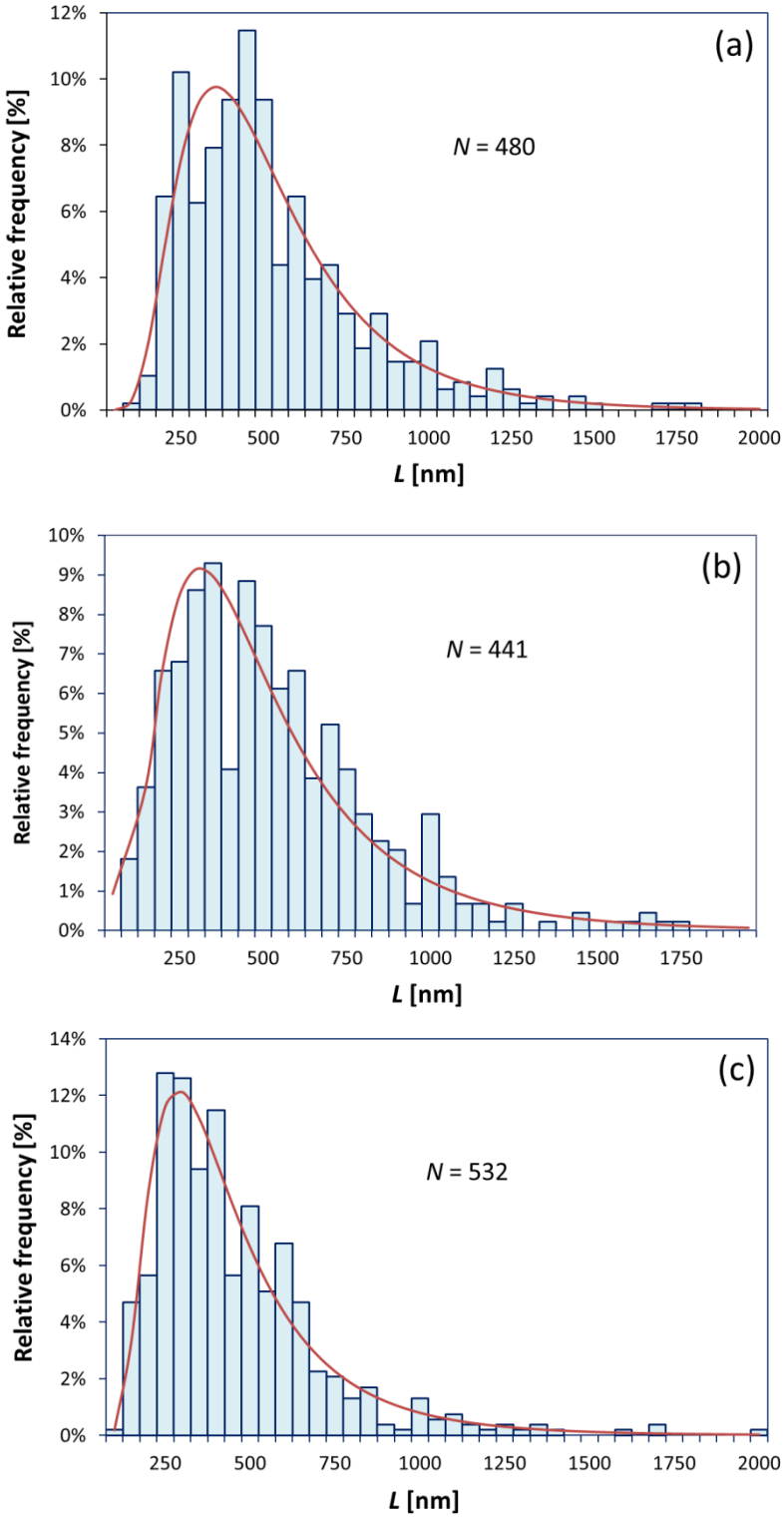

Figure S11. Histograms and fittings from SEM images of the CNT samples: a) MWCNT, b) CVD-SWCNT, and c) AD-SWCNT.

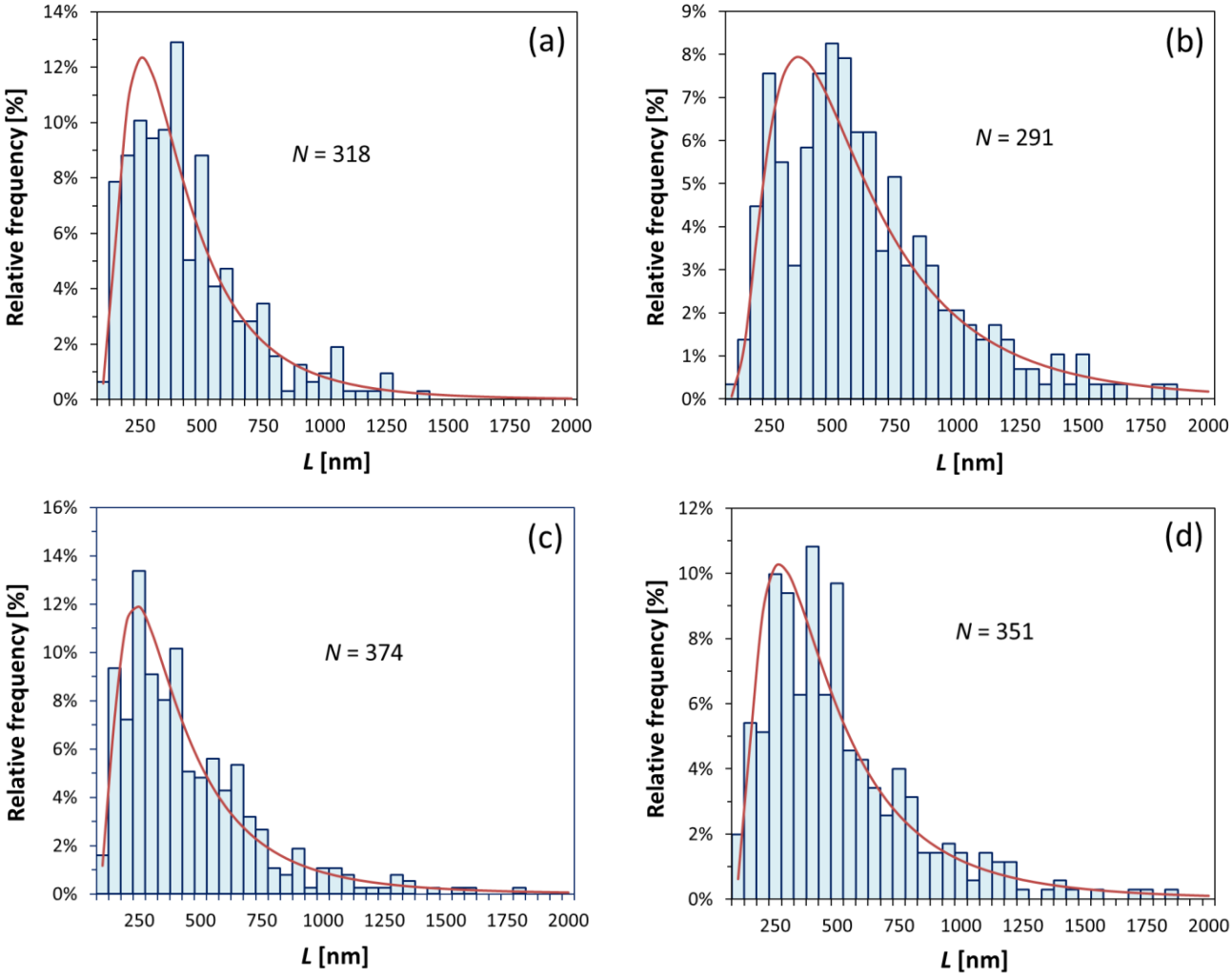

Figure S12. Histograms and fittings from SEM images of the functionalized MWCNT samples: a) c-HNO_3-MWCNT, b) d-HNO_3-MWCNT, c) F-MWCNT, and d) HSO_3-MWCNT.

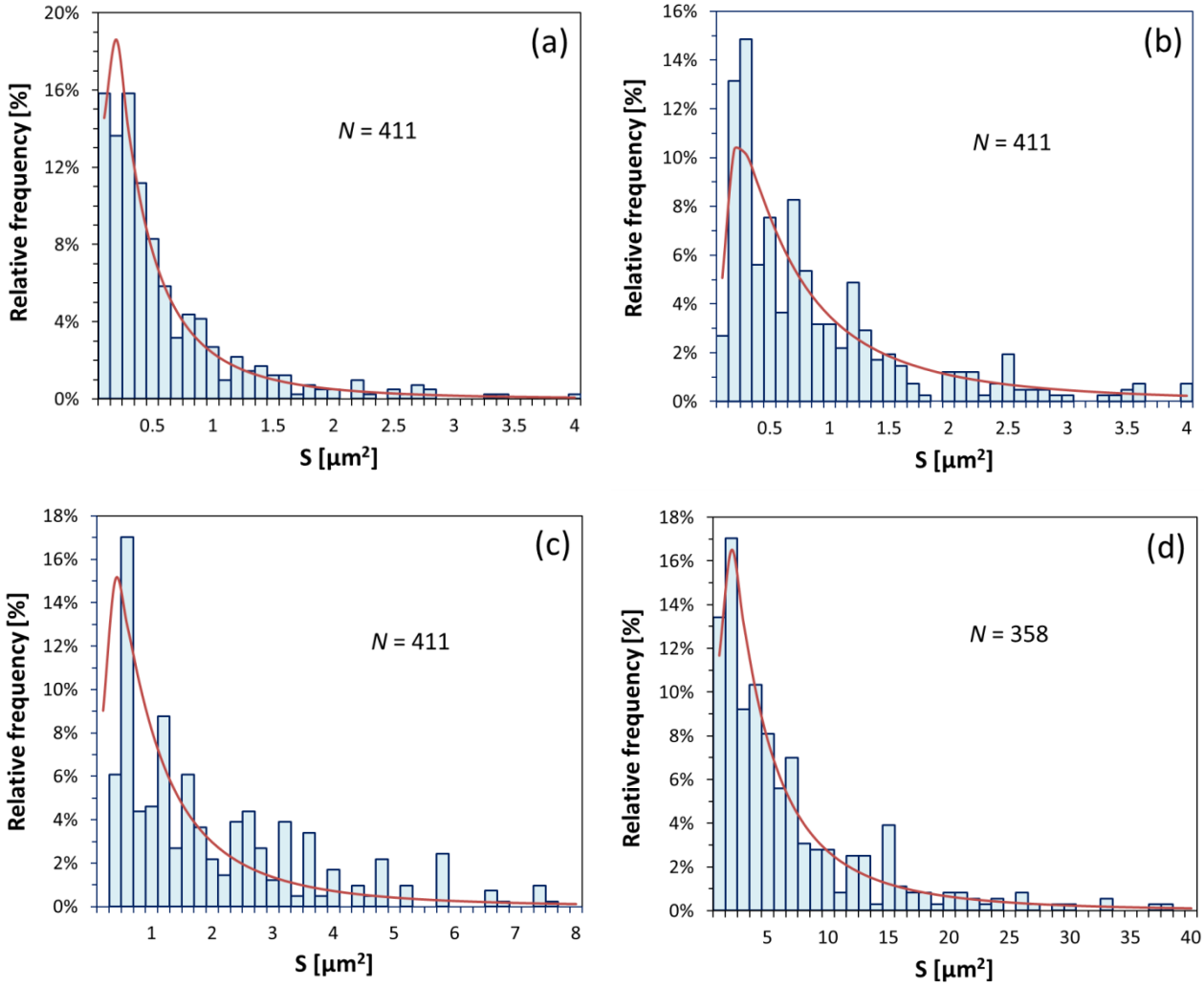

Figure S13. Histograms and fittings from SEM images of the GO samples: a) GO-2, b) GO-4, c) GO-16, and d) GO-G.

S11. X-ray diffraction experiments

Powder X-ray diffraction (XRD) of freeze-dried GO samples (Figure S14) was performed at room temperature on a Bruker AXS D8 Advance diffractometer using CuKα radiation. The peak at around $2\theta \approx 10^{o}$ was analyzed for the calculation of d_{LL} and the flake thickness (equivalently the n_{LL} value) by means of the Bragg and Scherrer equations respectively.

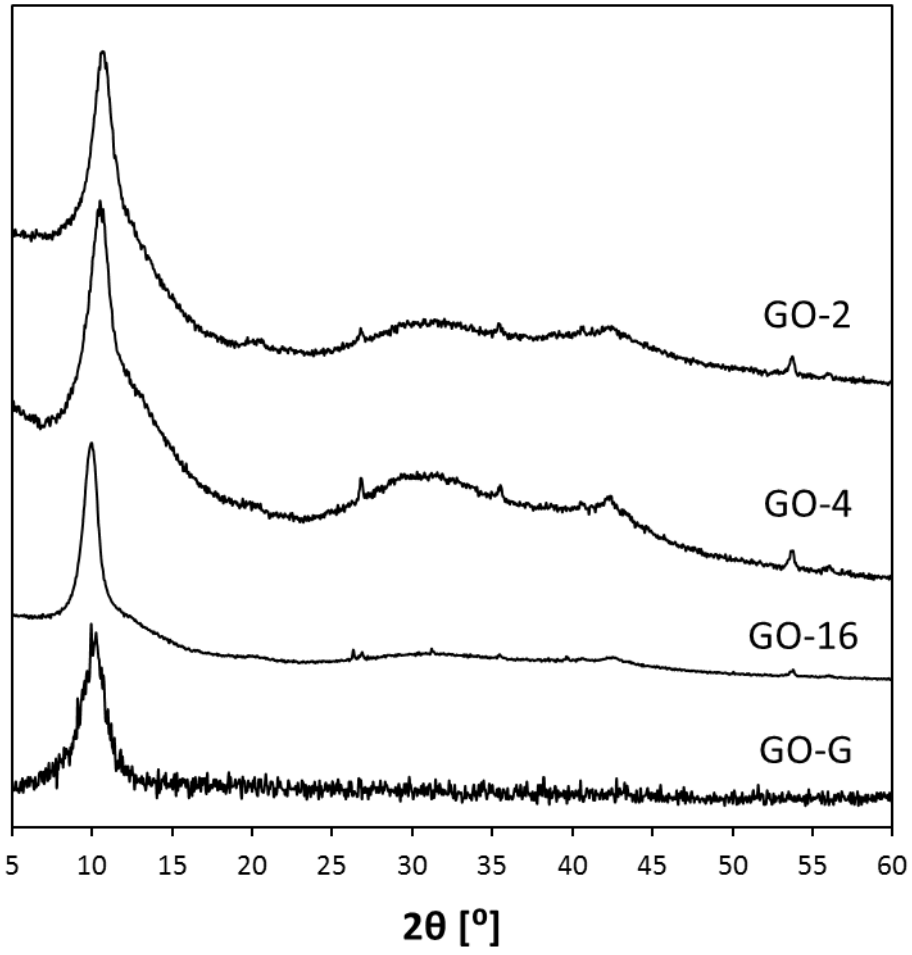

Figure S14. XRD patterns of freeze-dried GO powders.

S12. Chemical functionalization of MWCNTs

The c-HNO_3-MWCNT and d-HNO_3-MWCNT materials were prepared by refluxing MWCNTs in 9.5M HNO_3 for 18h and 1.5M HNO_3 for 2h respectively (Ref. 53).

Functionalization with heptadecafluorooctyl phenyl groups for the preparation of the F-MWCNT material was accomplished by reaction with the corresponding *in situ* generated diazonium compound (Ref 52). 250 mg of MWCNTs was tip sonicated in 50 mL of N,N'-dimethylformamide (DMF) for 60 min. Separately, 460 mg of 4-heptadecafluorooctyl aniline (Sigma-Aldrich 28623) were dissolved in 50 mL of acetonitrile and added to the CNT dispersion. The mixture was heated to 60ºC under constant magnetic stirring, and then 2 mL of isoamyl nitrite was added. The reaction mixture was left overnight at 60ºC, vacuum filtered through a 0.1 µm Teflon membrane and washed with DMF and methanol.

Similarly, the preparation of the HSO_3-MWCNT material was accomplished through the reaction with the appropriate aniline (Ref. 10). 50 mg of MWCNTs were dispersed in DMF, aided by ultrasonication (5-10 min), at a concentration of 1 $mg \cdot mL^{-1}$. Next, 1.2 equivalents (per mol of C) of 4-aminobenzenesulfonic acid were incorporated, and the system was stabilized at 80 °C. Afterwards, 3.2 equivalents of isopentyl nitrite per equivalent of aniline were dropwise incorporated in the system and the mixture was allowed to react at 80 °C for 1 h. The whole reaction medium was then filtered and rinsed with DMF until no color was observed to fall down. The functionalized MWCNTs were collected and re-dispersed in DMF. This was again filtered in equal conditions, and the process was repeated until obtaining a persistently colorless filtrate. This washing sequence was continued in identical manner with alternant cycles of Milli-Q water and DMF, then methanol, and finally the filtered solid sample was rinsed in the filter with diethyl ether and left to dry at room temperature under vacuum.